

Growth and photoluminescence studies of Al-rich AlN/Al_xGa_{1-x}N quantum wells

T. M. Al Tahtamouni, N. Nepal, J. Y. Lin, and H. X. Jiang^{a)}

Department of Physics, Kansas State University, Manhattan, Kansas 66506-2601

W. W. Chow

Semiconductor Material and Device Sciences Department, Sandia National Laboratories, Albuquerque, New Mexico 87185-0601

(Received 4 April 2006; accepted 11 August 2006; published online 29 September 2006)

A set of AlN/Al_xGa_{1-x}N ($x \sim 0.65$) quantum wells (QWs) with well width L_w varying from 1 to 3 nm has been grown by metal organic chemical vapor deposition. Low temperature photoluminescence (PL) spectroscopy has been employed to study the L_w dependence of the PL spectral peak position, emission efficiency, and linewidth. These results have shown that these AlN/AlGa_xN QW structures exhibit polarization fields of ~ 4 MV/cm. Due to effects of quantum confinement and polarization fields, AlN/AlGa_xN QWs with L_w between 2 and 2.5 nm exhibit the highest quantum efficiency. The dependence of the emission linewidth on L_w yielded a linear relationship. The implications of our results on deep ultraviolet optoelectronic device applications are also discussed. © 2006 American Institute of Physics. [DOI: 10.1063/1.2358107]

Deep ultraviolet (UV) emitters and detectors operating in the 200–340 nm wavelength range are important devices for many applications, including water purification, biochemical agent detection, medical research/health care, and high-density data storage.¹ Al-rich AlGa_xN alloys have the capability of emitting at short wavelengths down to 210 nm, which makes them very useful for these applications. As demonstrated by light emitting diodes, laser diodes, and electronic devices, many III-nitride based devices must take advantage of quantum-well (QW) structures in order to achieve optimal device performance. To realize deep UV emission ($\lambda < 280$ nm), Al-rich AlGa_xN based QWs are required. Recently, several groups have been studying Al-rich AlGa_xN-based emitters to obtain UV emission wavelength below 300 nm.^{2–8} However, the quantum efficiency (QE) of these deep UV emitters is presently very low. Systematic studies of Al-rich Al_xGa_{1-x}N alloys and AlN/Al_xGa_{1-x}N QWs are needed in order to probe the underlying mechanisms and necessary layer structural designs for providing improved QE.

In this study, a set of AlN/Al_{0.65}Ga_{0.35}N QWs with well width (L_w) varying from 1 to 3 nm and a fixed barrier width of 10 nm has been grown by metal organic chemical vapor deposition (MOCVD). Deep UV PL emission spectroscopy has been employed to probe the L_w dependence of the optical properties. Our results revealed that the highest QE could be obtained in QWs with L_w between 2 and 2.5 nm. The estimated value of the polarization fields (piezoelectric and spontaneous fields) induced in the well regions was found to be around 4 MV/cm, which agrees reasonably well with the calculations. A linear relationship between the emission linewidth and L_w has also been observed.

AlN/Al_xGa_{1-x}N ($x \sim 0.65$) QW samples were grown on sapphire (0001) substrates by MOCVD. The growth temperature and pressure were 1150 °C and 100 Torr, respectively. For each of the five samples, prior to the growth of

Al_{0.65}Ga_{0.35}N QW, a thin AlN buffer layer and a 1 μm undoped AlN epilayer were grown on the sapphire substrate. It was then followed by the growth of Al_{0.65}Ga_{0.35}N QW and a 10 nm AlN barrier. The targeted L_w of these samples were 1, 1.5, 2, 2.5, and 3 nm. The barrier and well widths were determined by the growth rates of the AlN and Al_xGa_{1-x}N epilayers.

The samples were mounted on a low temperature (10 K) stage with a cold finger in a closed-cycle helium refrigerator. The deep UV PL spectroscopy system consists of a frequency quadrupled 100 fs Ti:sapphire laser with an average power of 3 mW and repetition rate of 76 MHz at 196 nm and a 1.3 m monochromator with a detection capability ranging from 185 to 800 nm.⁹

The cw PL spectra of these five samples measured at 10 K are shown in Fig. 1. The dominant PL emission lines are due to the localized exciton recombination in the AlGa_xN QW regions.^{10,11} With respect to the band edge transition at 4.969 eV in Al_{0.65}Ga_{0.35}N epilayers, the PL peak energy is

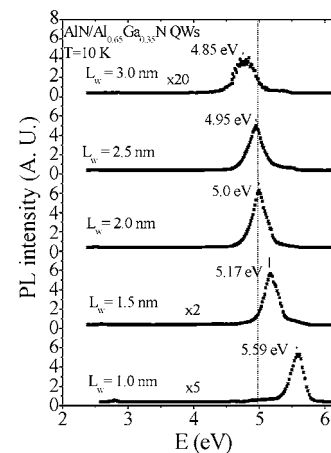


FIG. 1. Low temperature (10 K) PL spectra of AlN/Al_{0.65}Ga_{0.35}N QW samples with well width varying from 1 to 3 nm and a fixed barrier width of 10 nm. The vertical dashed line represents the emission peak position of Al_{0.65}Ga_{0.35}N epilayers.

^{a)}Electronic mail: jiang@phys.ksu.edu

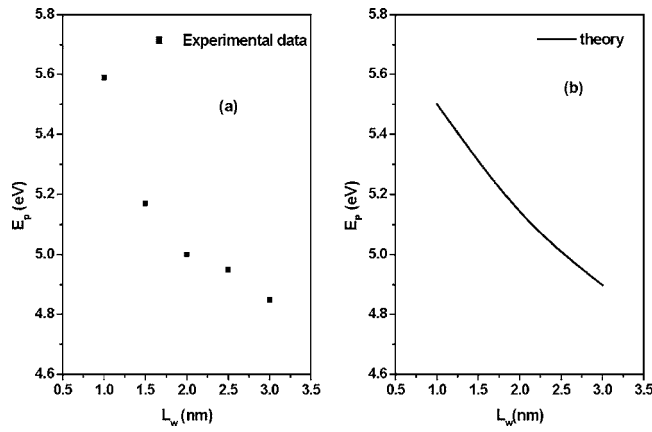


FIG. 2. (a) PL emission energy peak position (E_p) vs well width (L_w) for AlN/Al_{0.65}Ga_{0.35}N QWs measured at 10 K. (b) The calculated curve of E_p vs L_w by taking the spontaneous polarization and piezoelectric fields into account.

redshifted for QWs with $L_w = 2.5$ and 3 nm and blueshifted for QWs with $L_w = 1, 1.5$, and 2 nm. This indicates that the PL peak energy is defined by the quantum confinement as well as by the induced fields (piezoelectric and spontaneous fields) along the growth direction.¹² In order to find out the polarization fields in the QWs, we calculate emission peak positions for QWs with different well widths. The calculation begins with the determination of quantum-well band structure properties by simultaneously diagonalizing the $k \cdot p$ Hamiltonian and solving Poisson's equation.¹³ The input parameters are the bulk material parameters, where for AlGa_xN, we use the weighted averages of AlN and GaN values. Using the quantum-well band structure information, we numerically solve the semiconductor Bloch equations for the steady state microscopic polarization.¹⁴ The many-body effects appear as carrier density dependences in the transition energy and Rabi frequency. Carrier-carrier correlations, which lead to screening and dephasing, are treated at the level of quantum kinetic theory in the Markovian limit. The steady state polarization at an input laser field and carrier density (assuming quasiequilibrium condition) gives the linear absorption spectrum. The corresponding spontaneous emission spectrum is obtained using phenomenological relationship that relates the spontaneous emission and absorption spectra.¹⁵ The emission peak energies are then extracted from the spectra.

Figure 2(a) plots the PL spectral peak position, E_p , as a function of L_w . The curve in Fig. 2(b) is the theoretical curve of E_p as a function of L_w from which we deduce the value of the polarization fields to be around 4 MV/cm. The value of the polarization field (F) in the well region can also be calculated using the equation¹²

$$F = \frac{L_b(P_{\text{tot}}^b - P_{\text{tot}}^w)}{[\epsilon_0(L_w\epsilon_b + L_b\epsilon_w)]}, \quad (1)$$

where $\epsilon_{b,w}$ being the relative dielectric constant of barrier and well materials, $P_{\text{tot}}^{b,w}$ is the total polarization (piezoelectric plus spontaneous) in barrier and well, and L_b is the barrier width. The piezoelectric polarization can be calculated as $P_{\text{piezo}} = -[2e_{31} - 2(c_{13}e_{33}/c_{33})]\epsilon_{xx}$, where e_{ij} are the piezoelectric constants, C_{ij} are the elastic constants, and ϵ_{xx} is the in plane strain. To calculate the value of the polarization fields in the Al_xGa_{1-x}N well, we used the parameters given in Ref. 16 assuming a linear relationship between the GaN and AlN

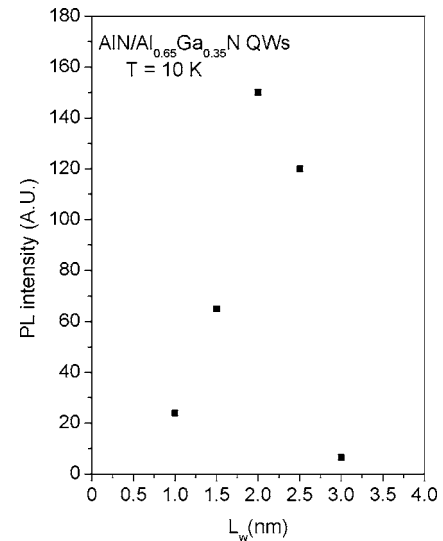


FIG. 3. Integrated PL emission intensity vs well width of AlN/Al_{0.65}Ga_{0.35}N QWs measured at 10 K.

values to extract the values for Al_xGa_{1-x}N alloys. The calculated value of the polarization fields from Eq. (1) ranges between 3.96 and 3.37 MV/cm depending on the well width, which is in reasonable agreement with the deduced value.

The integrated PL emission intensity versus L_w measured at 10 K for these AlN/Al_{0.65}Ga_{0.35}N QWs is plotted in Fig. 3, which shows that the highest QE is achieved when L_w is between 2 and 2.5 nm. The PL intensity depends strongly on the L_w . The reason for the rapid reduction of the emission intensity with the increase of L_w can be attributed to the reduction of the radiative recombination rate¹⁷ (or QE) due to the polarization fields in the well, which increases the spatial separation of electron and hole wave functions with increasing L_w .^{18,19} On the other hand, the decreased emission intensity with L_w (for small well width $L_w < 2$ nm) is due to the enhanced carrier leakage to the barrier region.¹⁷ From Fig. 1, the emission linewidths of these AlN/Al_xGa_{1-x}N QWs are fairly large. A similar trend was observed for GaN/InGa_xN QWs. The broad linewidth of GaN/InGa_xN has been explained in terms of In compositional fluctuation.^{20,21} For AlN/Al_xGa_{1-x}N QWs in addition to compositional fluctuation, polarization fields have to be taken into account to analyze the emission linewidth of the QWs. The effective transition energy in QWs under the influence of a piezoelectric field is given by²²

$$E = E_g + E_{\text{con}} - eFL_w, \quad (2)$$

where E_g is the band gap of the well material, E_{con} is the confinement energy, and eFL_w is due to the polarization field effect. In the first order approximation, the variation of the emitted photon energy (i.e., the linewidth) is given by the sum of fluctuations in the band gap of the well material, the confinement energy, the polarization fields, and the L_w .

$$\delta E = \delta E_g + \delta E_{\text{con}} + eL_w\delta F + eF\delta L_w. \quad (3)$$

Neglecting the variation of the confinement energy δE_{con} in cases of QWs with well width larger than the Bohr radius of excitons (i.e., about 1.3 nm), Eq. (3) can be written in terms of the dependence on L_w as follows:

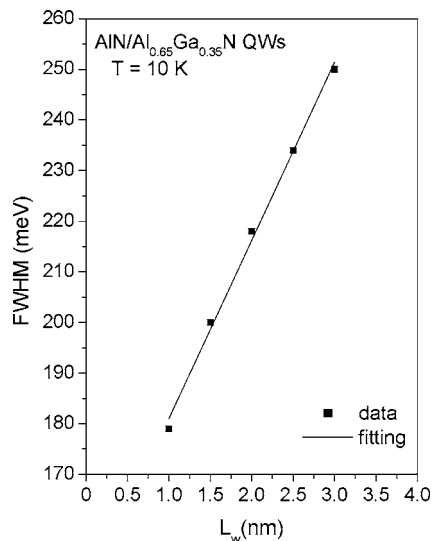


FIG. 4. Variation of the full width at half maximum (FWHM) of the PL emission spectra with well width for AlN/Al_{0.65}Ga_{0.35}N QWs measured at 10 K. The solid line is the linear fit of the experimental data.

$$\delta E = (\delta E_g + eF \delta L_w) + (e \delta F) L_w. \quad (4)$$

This equation reveals a linear relation between the linewidth and L_w with assumption that the well width fluctuation (δL_w) is fixed for all QWs and is about 1 ML (~ 0.5 nm). Figure 4 shows the variation of the full width at half maximum (FWHM) of the emission spectra of AlN/Al_{0.65}Ga_{0.35}N QWs with L_w measured at 10 K. FWHM increases linearly with increasing L_w . The solid line is a linear fit of the experimental data with Eq. (4). A localization energy around 100 meV is extracted which is consistent with the previously reported values in Al_xGa_{1-x}N epilayers.²³ Assuming that the well width fluctuation is 1 ML (~ 0.5 nm), another 35 meV is extracted. Thus the large emission linewidth of the AlN/Al_xGa_{1-x}N QWs can be well explained by the effects of alloy fluctuation and polarization fields.

In summary, a set of AlN/Al_{0.65}Ga_{0.35}N QWs with L_w varying from 1 to 3 nm has been grown by MOCVD. A systematic dependence of the PL emission peak position on L_w was observed, from which a value of ~ 4 MV/cm for the polarization fields in AlN/Al_{0.65}Ga_{0.35}N QWs was deduced. The PL emission linewidth was found to increase linearly with L_w . Furthermore, our results have shown that highest

QE was obtained in AlN/Al_{0.65}Ga_{0.35}N QWs with well width between 2 and 2.5 nm, which will serve as a guideline for designing optimal deep UV light emitter structures.

This research is supported by NSF and ARO.

- ¹C. J. Collins, A. V. Sampath, G. A. Garrett, W. L. Saeney, H. Shen, M. Wraback, A. Yu. Nikiforov, G. S. Cargill, and V. Dierolf, *Appl. Phys. Lett.* **86**, 031916 (2005).
- ²H. Hirayama, Y. Enomoto, A. Kinoshita, A. Hirata, and Y. Aoyagi, *Appl. Phys. Lett.* **80**, 37 (2001).
- ³V. Adivarahan, S. Wu, J. P. Zhang, A. Chitnis, M. Shatalov, V. Mandavilli, R. Gaska, and M. Asif Khan, *Appl. Phys. Lett.* **84**, 4762 (2004).
- ⁴J. P. Zhang, A. Chitnis, V. Adivarahan, S. Wu, V. Mandavilli, R. Pachipulusu, M. Shatalov, G. Simin, J. W. Yang, and M. Asif Khan, *Appl. Phys. Lett.* **81**, 4910 (2002).
- ⁵A. Yasan, R. McClintock, K. Mayes, D. Shiell, L. Gautero, S. R. Darvish, P. Kung, and M. Razeghi, *Appl. Phys. Lett.* **83**, 4701 (2003).
- ⁶A. Hanlon, P. M. Pattison, J. F. Kaeding, R. Sharma, P. Fini, and S. Nakamura, *Jpn. J. Appl. Phys., Part 2* **42**, L628 (2003).
- ⁷A. J. Fischer, A. A. Allerman, M. H. Crawford, K. H. A. Bogart, S. R. Lee, R. J. Kaplar, W. W. Chow, S. R. Kurtz, K. W. Fuller, and J. J. Figiel, *Appl. Phys. Lett.* **84**, 3394 (2004).
- ⁸S. Wu, V. Adivarahan, M. Shatalov, A. Chitnis, W. Sun, and M. Asif Khan, *Jpn. J. Appl. Phys., Part 2* **43**, L1035 (2004).
- ⁹<http://www.phys.ksu.edu/area/GaNgroup>
- ¹⁰H. S. Kim, R. A. Mair, J. Li, J. Y. Lin, and H. X. Jiang, *Appl. Phys. Lett.* **76**, 1252 (2000).
- ¹¹G. Coli, K. K. Bajaj, J. Li, J. Y. Lin, and H. X. Jiang, *Appl. Phys. Lett.* **78**, 1829 (2001); **80**, 2907 (2002).
- ¹²A. Bonfiglio, M. Lomascolo, R. Cingolani, A. Di Carlo, F. Della Sala, P. Lugli, A. Botchkarev, and H. Morkoc, *J. Appl. Phys.* **87**, 2289 (1999).
- ¹³J. Wang, J. B. Jeon, M. Sirenko, and K. W. Kim, *IEEE Photonics Technol. Lett.* **9**, 728 (1997).
- ¹⁴W. Chow, M. Kira, and S. W. Koch, *Phys. Rev. B* **60**, 1947 (1999).
- ¹⁵C. H. Henry, R. A. Logan, and F. R. Merritt, *J. Appl. Phys.* **51**, 3042 (1980).
- ¹⁶I. Vurgaftman, J. R. Meyer, and L. R. Ram-Mohan, *J. Appl. Phys.* **89**, 5815 (2001).
- ¹⁷K. C. Zeng, J. Li, J. Y. Lin, and H. X. Jiang, *Appl. Phys. Lett.* **76**, 3040 (2000).
- ¹⁸S. H. Park and S. L. Chuang, *Appl. Phys. Lett.* **72**, 3103 (1998).
- ¹⁹J. S. Im, H. Kollmer, J. Off, A. Sohmer, F. Scholtz, and A. Hangleiter, *Phys. Rev. B* **57**, R9435 (1998).
- ²⁰S. Chichibu, T. Azuhata, T. Sota, and S. Nakamura, *Appl. Phys. Lett.* **69**, 4188 (1996).
- ²¹A. Satake, Y. Masumoto, T. Miyajima, T. Asatsuma, F. Nakamura, and M. Ikeda, *Phys. Rev. B* **57**, R2041 (1998).
- ²²C. Bodin, R. Andre, J. Cibert, Le Si Dang, D. Bellet, G. Feuillet, and P. H. Jouneau, *Phys. Rev. B* **51**, 13181 (1995).
- ²³N. Nepal, J. Li, M. L. Nakarmi, J. Y. Lin, and H. X. Jiang, *Appl. Phys. Lett.* **88**, 062103 (2006).